Highly Selective CO2 Capture on Waste Polyurethane Foam-Based Activated Carbon

Authors:

Chao Ge, Dandan Lian, Shaopeng Cui, Jie Gao, Jianjun Lu

Date Submitted: 2019-11-24

Keywords: ultra-micropore, Carbon Dioxide Capture, high selectivity, physical activation, waste polyurethane foam

Abstract:

Low-cost activated carbons were prepared from waste polyurethane foam by physical activation with CO2 for the first time and chemical activation with Ca(OH)2, NaOH, or KOH. The activation conditions were optimized to produce microporous carbons with high CO2 adsorption capacity and CO2/N2 selectivity. The sample prepared by physical activation showed CO2/N2 selectivity of up to 24, much higher than that of chemical activation. This is mainly due to the narrower microporosity and the rich N content produced during the physical activation process. However, physical activation samples showed inferior textural properties compared to chemical activation samples and led to a lower CO2 uptake of 3.37 mmol·g?1 at 273 K. Porous carbons obtained by chemical activation showed a high CO2 uptake of 5.85 mmol·g?1 at 273 K, comparable to the optimum activated carbon materials prepared from other wastes. This is mainly attributed to large volumes of ultra-micropores (<1 nm) up to 0.212 cm3·g?1 and a high surface area of 1360 m2·g?1. Furthermore, in consideration of the presence of fewer contaminants, lower weight losses of physical activation samples, and the excellent recyclability of both physical- and chemical-activated samples, the waste polyurethane foam-based carbon materials exhibited potential application prospects in CO2 capture.

Record Type: Published Article

Submitted To: LAPSE (Living Archive for Process Systems Engineering)

Citation (overall record, always the latest version):	LAPSE:2019.1181
Citation (this specific file, latest version):	LAPSE:2019.1181-1
Citation (this specific file, this version):	LAPSE:2019.1181-1v1

DOI of Published Version: https://doi.org/10.3390/pr7090592

processes

MDPI

Article

Highly Selective CO_2 Capture on Waste Polyurethane Foam-Based Activated Carbon

Chao Ge [1], Dandan Lian [1], Shaopeng Cui [2], Jie Gao [3] and Jianjun Lu [1,4,*]

1 College of Textile Engineering, Taiyuan University of Technology, Jinzhong 030600, China
2 College of Forestry, Shanxi Agricultural University, Taigu 030801, China
3 State Key Laboratory of Coal Conversion, Institute of Coal Chemistry, Chinese Academy of Sciences, Taiyuan 030001, China
4 Key Laboratory of Coal Science and Technology, Taiyuan University of Technology, Taiyuan 030024, China
* Correspondence: lujianjunktz@tyut.edu.cn; Tel.: +86-0351-3176-555

Received: 8 August 2019; Accepted: 28 August 2019; Published: 3 September 2019

Abstract: Low-cost activated carbons were prepared from waste polyurethane foam by physical activation with CO_2 for the first time and chemical activation with $Ca(OH)_2$, NaOH, or KOH. The activation conditions were optimized to produce microporous carbons with high CO_2 adsorption capacity and CO_2/N_2 selectivity. The sample prepared by physical activation showed CO_2/N_2 selectivity of up to 24, much higher than that of chemical activation. This is mainly due to the narrower microporosity and the rich N content produced during the physical activation process. However, physical activation samples showed inferior textural properties compared to chemical activation samples and led to a lower CO_2 uptake of 3.37 $mmol \cdot g^{-1}$ at 273 K. Porous carbons obtained by chemical activation showed a high CO_2 uptake of 5.85 $mmol \cdot g^{-1}$ at 273 K, comparable to the optimum activated carbon materials prepared from other wastes. This is mainly attributed to large volumes of ultra-micropores (<1 nm) up to 0.212 $cm^3 \cdot g^{-1}$ and a high surface area of 1360 $m^2 \cdot g^{-1}$. Furthermore, in consideration of the presence of fewer contaminants, lower weight losses of physical activation samples, and the excellent recyclability of both physical- and chemical-activated samples, the waste polyurethane foam-based carbon materials exhibited potential application prospects in CO_2 capture.

Keywords: waste polyurethane foam; physical activation; high selectivity; CO_2 capture; ultra-micropore

1. Introduction

CO_2 emission from the combustion of coal and natural gas is mainly responsible for global warming [1,2]. The "least-cost" solution is to limit greenhouse gas emissions to meet the Paris Agreement pledges, wherein 60% of CO_2 emissions are hoped to be reduced in 2030 relative to 2005 [3]. To reduce the emission of CO_2, the selective and energy-efficient capture and storage of CO_2 is considered to be a satisfactory approach. Until now, three main CO_2 capturing strategies, namely pre-combustion, post-combustion, and oxy-combustion, have been discussed. For pre-combustion, the coal must be gasified first; the typical technology used is called an integrated gasification combined cycle. Post-combustion involves capturing CO_2 from the flue gases produced after fossil fuels are burned. Both of these methods have been widely accepted and used in gas-stream purification in industry. Oxy-combustion can produce a relatively pure CO_2 stream in emissions, but it is still in development due to the high cost of the technology involved [4]. In addition to these, several technologies have also been investigated to separate and store CO_2, such as membrane separation, solution absorption, cryogenic refrigeration, and adsorption approaches [5–7]. Although these CCUS

(Carbon Capture, Utilization and Storage) technologies are intended to reduce CO_2 emission, reaching the Paris Agreement targets is still a serious challenge. Nevertheless, in these techniques, adsorption is considered to be the approach with the most potential, since it involves simple operation and has low-cost and energy-saving benefits [8].

Many adsorbents have been intensively studied for CO_2 capture, including zeolites [9], metal-organic frameworks [10], metallic oxide [11], graphene-based adsorbents [12], and porous carbon materials [13]. For future commercialization application, the selection of adsorbents is strongly dependent not only on CO_2 capture capacity but also the cost, including the availability of the raw materials, the preparation of the adsorbent, and the operating costs. Porous carbons (PCs) are considered to be the most competitive candidates due to their controlled pore structure, low cost, stable physicochemical properties, ease of chemical modification, and regeneration [14]. Micropore sizes smaller than 1 nm are beneficial to high-density CO_2 filling at ambient conditions [15,16]. In addition, a high surface area (>1000 $m^2 \cdot g^{-1}$) and a rich nitrogen environment can improve the CO_2 adsorption capacity.

The route of preparation, especially activation, will significantly affect the performance of CO_2 absorption. The porous carbons can be activated either by physical or chemical methods. Physical activation is usually achieved by carbonization in an inert atmosphere followed by oxidizing in CO_2 [17], steam [18], or air. In this way, activated carbons with a narrower pore size distribution can be obtained [19]. Generally, chemical activation takes advantage of oxidizing or dehydrating agents, such as KOH [1,15,20], NaOH, H_3PO_4, or $CaCl_2$, and being subjected to calcination under N_2 between 773 and 1223 K. Chemical activation contributes to the formation of pores and lead to carbons with higher textural development. However, it is an energy-consuming process and is also associated with the corrosion of equipment and environmental problems [21].

To achieve green and sustainable development, the production of low-cost porous carbons from original waste materials is a good, established technique [22]. Polyurethane foams (PUFs), as one of the most important thermoset polymers, are widely used in the chemical industry, electronics, textiles, and medical and other fields due to their high strength, excellent wear resistance, and wide hardness range. The total annual production of polyurethane products in the Asia Pacific region was about 11.5 million tons in 2014, and it is predicted to be over 15.5 million tons by 2019 [23]. As a result, large amounts of useless waste and spent product were generated. Since the processes used for recycling polyurethane foams, like mechanical recycling [24] or chemical depolymerization [25,26], are highly time- and energy-consuming [27], most of the wastes are discarded in landfills or directly burnt, leading to serious environmental issues [28]. However, the ease of availability of the raw materials helps to make waste PUFs a potential activated carbon adsorbent. This would not only alleviate pollution and protect the environment, but it could also convert PUF into a high-value-added product.

Herein, low-cost activated carbons were prepared from waste PUF materials using physical activation with CO_2 for the first time, and chemical activation with metal hydroxide. The synthetic procedure is simple and clear, and production costs are low. The activation conditions, like physical activation temperature and chemical activating agent, were discussed and optimized to produce porous carbons with high CO_2 adsorption capacity and CO_2/N_2 selectivity. The richness of N content and narrower microporosity produced by physical activation may be responsible for the higher CO_2/N_2 selectivity of up to 24. Furthermore, physical activation leads to less contaminant and lower weight losses but also lower CO_2 uptake. Porous carbons obtained by chemical activation with KOH possess large volumes of micropores (<1 nm) and high surface areas of up to 0.212 $cm^3 \cdot g^{-1}$ and 1360 $m^2 \cdot g^{-1}$, respectively. This material exhibits a high CO_2 adsorption capacity of 5.85 $mmol \cdot g^{-1}$ at 273 K and excellent recyclability. The easy regeneration of the PUF-based carbon adsorbent requires minimum energy input, thus reducing operational costs. Therefore, the waste PUFs have the potential to be utilized for the production of activated carbon adsorbents on an industrial scale.

2. Materials and Methods

Prior to carrying out chemical or physical activation, a batch of waste PUFs were carbonized in a porcelain boat inside a horizontal tube furnace at 673 K for 1 h under nitrogen flow (60 mL·min^{-1}). The obtained material was designated as PUF/C. Chemical activation was conducted by treating the carbonized PUFs in alkaline solutions. First, 0.8 g PUF/C was dipped into 10 mL of separate aqueous solutions containing 1.6 g of $Ca(OH)_2$, NaOH, and KOH; was stirred uniformly for 1 h at room temperature; and was subsequently dried at 383 K for 12 h to remove water. Then, the mixture was heated up to 973 K under N_2 flow (60 mL·min^{-1}) for 2 h. The samples were thoroughly washed in diluted HCl and distilled water until pH = 7. The products were dried at 373 K for 6 h and denoted as PUF/C-$Ca(OH)_2$-973, PUF/C-NaOH-973, and PUF/C-KOH-973, respectively.

Physical activation of PUFs was accomplished by one-step carbonization and CO_2 activation. Certain amounts of PUFs were carbonized in the same procedure followed above, and then N_2 was switched to CO_2; the obtained PUF/C char was heated up to 1073–1273 K for 2 h under CO_2 flow (15 mL·min^{-1}). After physical activation, the sample was cooled to ambient temperature under nitrogen protection and was labeled as PUF/C-CO_2-x, where x represents the CO_2 activation temperature.

Nitrogen sorption isotherms and the textural properties of the porous carbons were measured at 77 K on an ASAP 2020 apparatus. Before N_2 adsorption measurements, all samples were degassed at 493 K for 4 h. The specific surface area was obtained using the BET method (p/p^0 = 0–0.5). The total pore volume was estimated with the amount of N_2 adsorbed at p/p_0 = 0.99. The morphology and structure of the obtained samples were investigated by scanning electron microscopy (SEM, JEOL JSM-700) and transmission electron microscopy (TEM, JEOL JEM-2001F). The amount of N in this paper was determined by elemental analysis using an Elemntar Vario EL Cube microanalyzer. X-ray photoelectron spectra (XPS) were collected on a Krato AXIS Ultra DLD spectrometer. CO_2 temperature-programmed-desorption (CO_2-TPD) was measured on a Micromeritics Autochem II 2920 chemisorption analyzer.

The CO_2 adsorption capacity and adsorption–desorption cycles were investigated at 273 K and ordinary pressure on a BEL-SORP-max instrument. The activated carbon materials were degassed at 453 K for at least 2 h before the measurement.

3. Results and Discussion

3.1. Pyrolysis of Wasted PUF and Morphologies of Activated Carbons

Figure 1 shows the pyrolysis of the waste polyurethane foam at a heating rate of 5 K·min^{-1} in a nitrogen atmosphere. Water adsorbed on the surface is released at about 373 K. The weight loss of the raw materials mainly occurs between 523–773 K, which include three differentiated weight loss peaks. The first peak nears 593 K, resulting from the formation of amines, methylene methyl, and methane species. The second peak around 653 K is due to the decomposition of isocyanate, and the third one near 733 K results from the production of quaternary N, aromatics, CH_4, and other species [15]. It is clear that the carbonized precursor mainly results from the former two peaks. Therefore, the carbonization temperature was subsequently set to 673 K.

Figure 2 shows the SEM and TEM images of carbonized and chemical and physical activation samples. A slightly rough surface appeared when the carbonized precursor was activated by $Ca(OH)_2$, but the activation degree was so limited that only few macropores existed on the surface (Figure 2b). In comparison, as it was activated by NaOH and KOH, the smooth surface changes to a multi-hole morphology to a large extent (Figure 2a,c,d). In addition, NaOH activation resulted in more macropores on the surface, while KOH activation led to the plentiful generation of micropores. These observations indicate that the carbonized precursor was etched increasingly severely by the chemical activation of $Ca(OH)_2$, NaOH, and KOH (Figure 2a–d). Furthermore, in the physical activation process, the activation temperature determines the development of porosity. It can be observed that the surface of the carbonized precursor became rugged after physical activation by CO_2 at 1173 K and formed

many micropores during the gasification reaction between CO_2 and carbon and the following diffusion processes of the generated products (Figure 2e,g). Micropore generation would possibly benefit the fast, dynamic CO_2 adsorption-desorption. Nevertheless, much higher physical activation temperatures should be avoided as they can broaden the average micropore width, producing few mesopores (Figure 2f,h), which is not good for CO_2 capture.

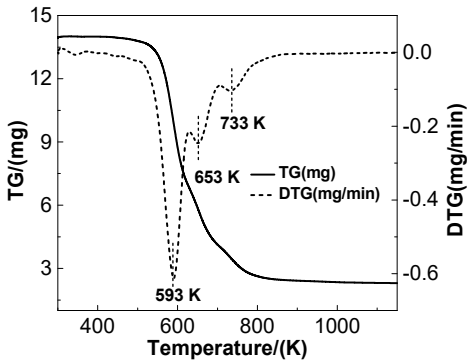

Figure 1. Pyrolysis of polyurethane foam measured at the heating rate of 5 K·min^{-1} in N_2 atmosphere.

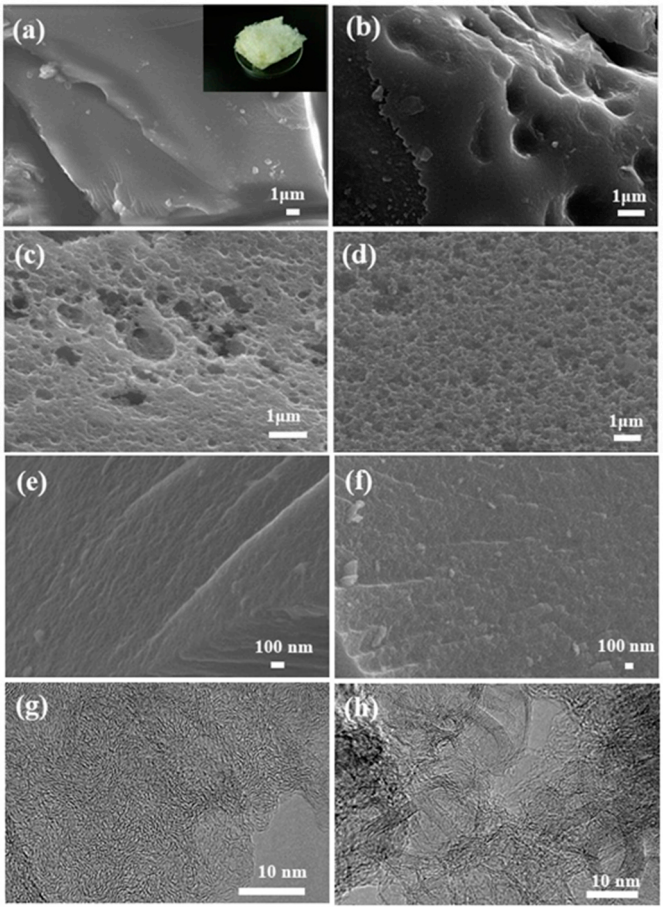

Figure 2. SEM images of the PUF/C (**a**), PUF/C-Ca(OH)$_2$-973 (**b**), PUF/C-NaOH-973 (**c**), PUF/C-KOH-973 (**d**), PUF/C-CO_2-1173 (**e**), PUF/C-CO_2-1273 (**f**), and TEM images of PUF/C-CO_2-1173 (**g**) and PUF/C-CO_2-1273 (**h**). The inset in (**a**) is a photo showing the morphology of waste polyurethane foams.

3.2. Surface Oxygen and Nitrogen Species Analyses

Figure 3 exhibits the FT-IR spectra of PUF-based activated carbons. The broad band around 3440 cm^{-1} could be ascribed to the N–H/O–H symmetric stretching vibration [29]. The intense

bands at 1090 cm^{-1} and 1584 cm^{-1} are related to C–O stretching [29] and N–H in-plane deformation. The relatively weak band around 1383 cm^{-1} is attributed to the C–N stretching vibration. Bands at 2927 and 2851 cm^{-1} could be ascribed to the C–H stretching vibrations of $–CH_2$ and $–CH_3$ [15]. The presence of oxygen and nitrogen species were further confirmed by XPS. The O 1s spectra show the presence of three main peaks at 531, 532.1, and 533.5 eV, which are attributed to –C=O, C–O–C/C–OH, and O–C=O, respectively (Figure 4) [30]. The results confirm that plentiful amounts of oxygen-rich functional groups are incorporated onto the surface of the PUF-based activated carbons, which play an important role in enhancing the overall CO_2 adsorption.

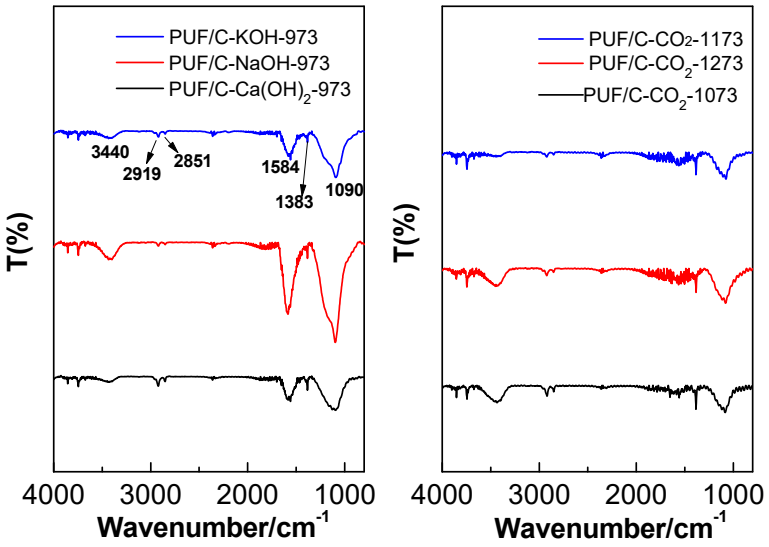

Figure 3. FT-IR spectra of the obtained samples prepared by physical and chemical activation.

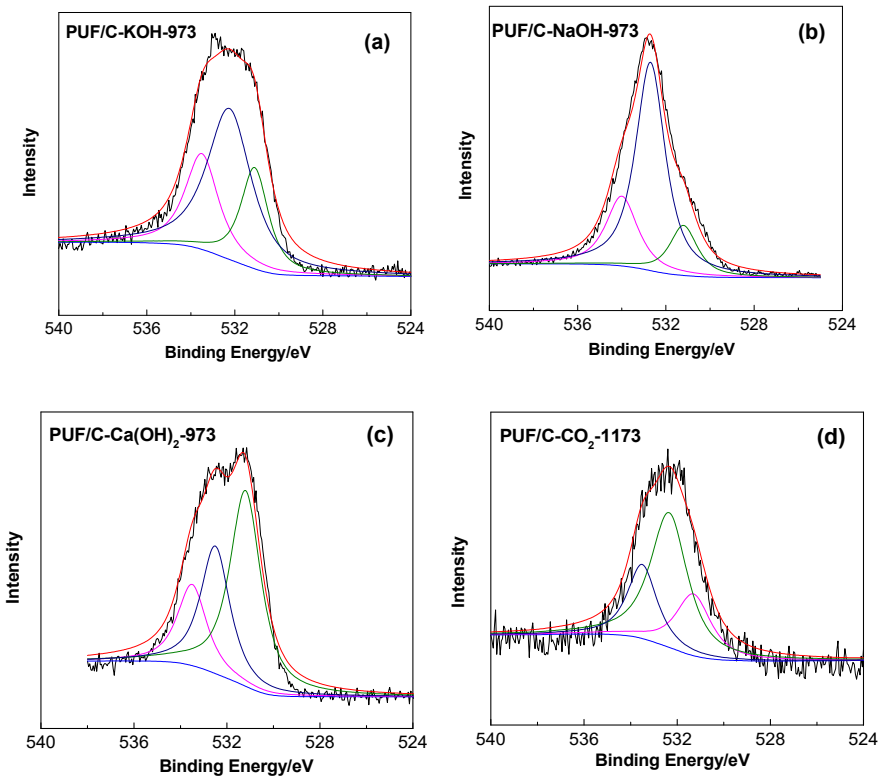

Figure 4. XPS spectra O 1s of PUF/C-KOH-973 (**a**), PUF/C-NaOH-973 (**b**), PUF/C-$Ca(OH)_2$-973 (**c**), and PUF/C-CO_2-1173 (**d**).

It is well-known that the type and content of N-containing species of carbon adsorbents can greatly affect CO_2 adsorption capacity. As shown in Figure 5, pyridinic (N-6), pyrrolic (N-5), quaternary N (N-Q), and pyridine N-oxide (N-X) species with binding energies of 398.5, 399.7, 400.9, and 403.0 eV, respectively, can be identified by deconvolving the N 1s signal of the activated carbons [31]. The specific components depend on the physical activation temperature or the degree of chemical activation with $R(OH)_x$ (R = Ca, Na, K; x = 1/2). The relative amount of pyridine N-oxide species increased with increasing CO_2 activation temperature. This can also apply to the quaternary N species (Figure 5a–c). Conversely, upon increasing the CO_2 activation temperature from 1073 to 1273 K, the contents of pyridinic and pyrrole N species dropped from 35% and 24% to 18% and 21%, respectively (Table 1), indicating that elevating the CO_2 activation temperature can decrease the total amount of N species and also convert the pyridinic nitrogen and pyrrole nitrogen to quaternary N and pyridine N-oxide species (Figure 5a–c). This trend was also observed upon increasing the degree of chemical activation using $Ca(OH)_2$, NaOH, and KOH as activated reagents (Figure 5d–f). The pyridinic and pyrrole-type N declined from 28% and 72% to 21% and 41%, respectively. Quaternary-N and pyridine N-oxide species are considered less effective in CO_2 capture than pyridinic and pyrrolic nitrogen [32], since basic N species are superior at capturing CO_2. Therefore, CO_2 uptake on the activated carbons would increase with decreasing the physical activation temperature or the degree of chemical activation under the conditions of similar porous structures. Actually, CO_2 uptake and physical activation temperature or the degree of chemical activation show a volcano relationship or a positive relationship, respectively, implying that the porous structure of the activated carbons may greatly affect their CO_2 capture.

Table 1. Surface nitrogen contents of polyurethane foam-based activated carbons prepared by physical and chemical activation.

Samples	Content (wt.%)				
	Total N [1]	N-6 [2]	N-5 [2]	N-Q [2]	N-X [2]
PUF/C-CO_2-1073	8.78	35	24	27	14
PUF/C-CO_2-1173	6.84	28	22	34	15
PUF/C-CO_2-1273	3.77	18	21	38	23
PUF/C-$Ca(OH)_2$-973	7.70	28	72	-	-
PUF/C-NaOH-973	7.51	20	60	-	20
PUF/C-KOH-973	6.92	21	41	22	16

[1] Determined by element analysis. [2] Relative content of different types of N species, as determined by XPS analysis results. pyridinic (N-6), pyrrolic (N-5), quaternary N (N-Q), and pyridine N-oxide (N-X) species.

Figure 6 shows the CO_2-TPD profiles of the porous carbons prepared by physical and chemical activation from wasted polyurethane foam. In general, physical and chemical adsorption are the two main routes for CO_2 capture. An intense peak was present between 343 and 358 K, indicating that most of the CO_2 molecules physically adsorbed on the activated carbons due to their developed pore structures. In contrast, a very weak peak was also observed around 448 K, implying that there exists a weak chemical interaction between CO_2 and N species. Thus, physical adsorption occupies the dominant position during the CO_2 capture process in this studied case.

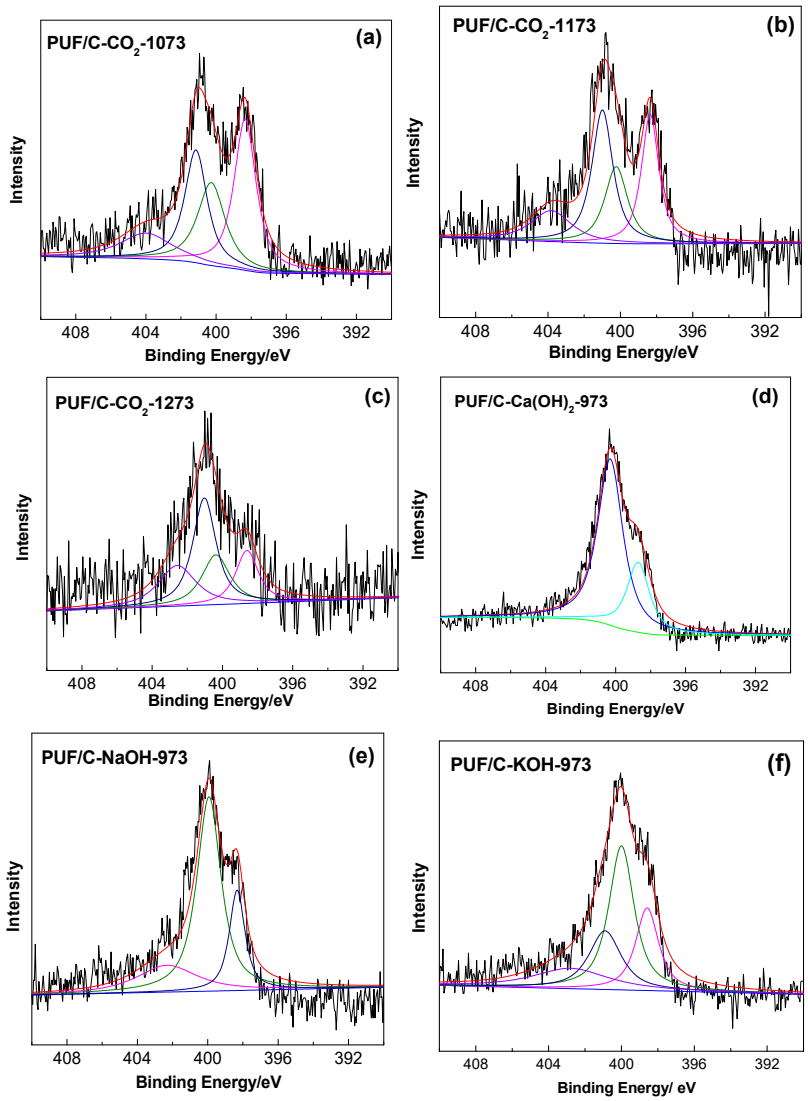

Figure 5. XPS N 1s spectra of PUF/C-CO_2-1073 (**a**), PUF/C-CO_2-1173 (**b**), and PUF/C-CO_2-1273 (**c**), PUF/C-$Ca(OH)_2$-973 (**d**), PUF/C-NaOH-973 (**e**), and PUF/C-KOH-973 (**f**).

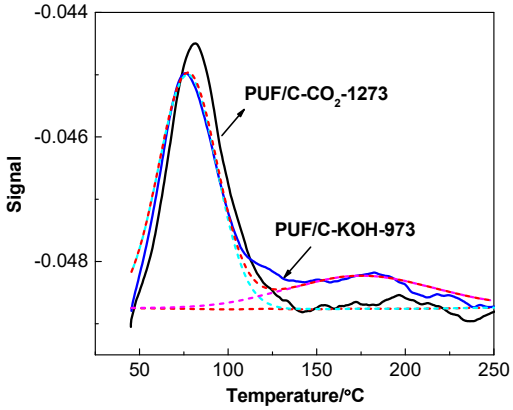

Figure 6. CO_2- temperature-programmed-desorption (TPD) profile of PUF/C-KOH-973 and PUF/C-CO_2-1273.

3.3. Effect of Physical and Chemical Activation on the Textural Properties of PUF-Based Porous Carbon Materials

Figure 7 shows the N_2 adsorption isotherms and pore size distributions (PSDs) of carbon materials after physical and chemical activation. Clearly, the prepared samples exhibit a typical micropore structure that is mainly responsible for CO_2 capture at ambient conditions [33]. Meanwhile, the hysteresis loops of the adsorption isotherm of PUF/C-KOH-973 or PUF/C-NaOH-973 are of type-IV, representing slit-shaped pores and implying the generation of mesopores (Figure 7a). It is well-known that carbon materials with narrow micropores can be obtained by physical activation [18]. It can be observed from Table 2 that, upon increasing CO_2 activation temperature from 1073 to 1273 K, the surface area and pore volume of the samples significantly rose from 15 $m^2 \cdot g^{-1}$ and 0.04 $cm^3 \cdot g^{-1}$ to 865 $m^2 \cdot g^{-1}$ and 0.42 $cm^3 \cdot g^{-1}$, respectively, and the PSDs (<1 nm) of samples widened from 0.58 to 0.87 nm (Figure 7b). In particular, the ultra-micropore (<1 nm) volume increased from 0.085 to 0.122 $cm^3 \cdot g^{-1}$ and then decreased to 0.119 $cm^3 \cdot g^{-1}$ upon elevating the activation temperature (Table 2 and Figure 8). A much higher physical activation temperature will make the reaction rate between carbon and CO_2 faster than the diffusion rate, which is not helpful for the formation of micropores. From the above, we can conclude that the pore structure of activated carbons could be controlled by adjusting the CO_2 activation temperature. In this work, the developed ultra-micropore can be obtained at 1173 K with a CO_2 flowrate of 15 $mL \cdot min^{-1}$.

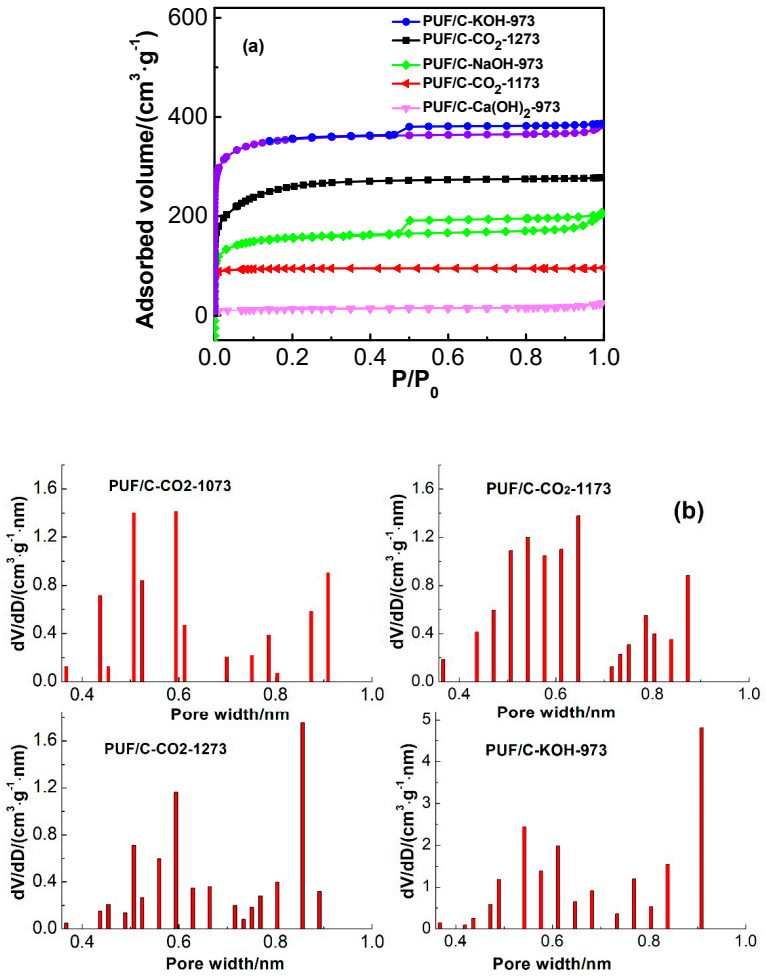

Figure 7. Adsorption isotherms of N_2 at 77 K (**a**) and pore size distributions determined by the Dubinin–Radushkevich equation applied to Table 2 adsorption data at 273 K (**b**) of the obtained samples prepared by physical and chemical activation.

Table 2. Textural parameters of prepared samples from adsorption isotherms of N_2 and CO_2.

Sample	Yield (%)	Textural Properties				
		N_2 Adsorption at 77 K			CO_2 Adsorption at 273 K	
		S_{BET} ($m^2 \cdot g^{-1}$)	V_t [1] ($cm^3 \cdot g^{-1}$)	V_{micro} [2] ($cm^3 \cdot g^{-1}$)	$V_{ultra\text{-}micro}$ [3] ($cm^3 \cdot g^{-1}$) (≤1 nm)	D [4] (nm)
PUF/C-CO_2-1073	16.0	15	0.04	0.03	0.085	0.58
PUF/C-CO_2-1173	14.0	206.7	0.10	0.08	0.122	0.64
PUF/C-CO_2-1273	9.3	865	0.42	0.11	0.119	0.87
PUF/C-$Ca(OH)_2$-973	25.5	39	0.04	0.01	-	-
PUF/C-NaOH-973	22.2	710	0.41	0.20	0.171	-
PUF/C-KOH-973	12.3	1360	0.59	0.52	0.212	0.91

[1] Total pore volume at $p/p_0 = 0.99$. [2] Micropore volume determined by the *t*-plot method. [3] The cumulative volume of pores smaller than 1 nm determined using CO_2 adsorption data at 273 K. [4] D is the maximum value of the PSDs. The yield of the prepared sample was calculated by the mass ratio of activated carbon and dry PUF.

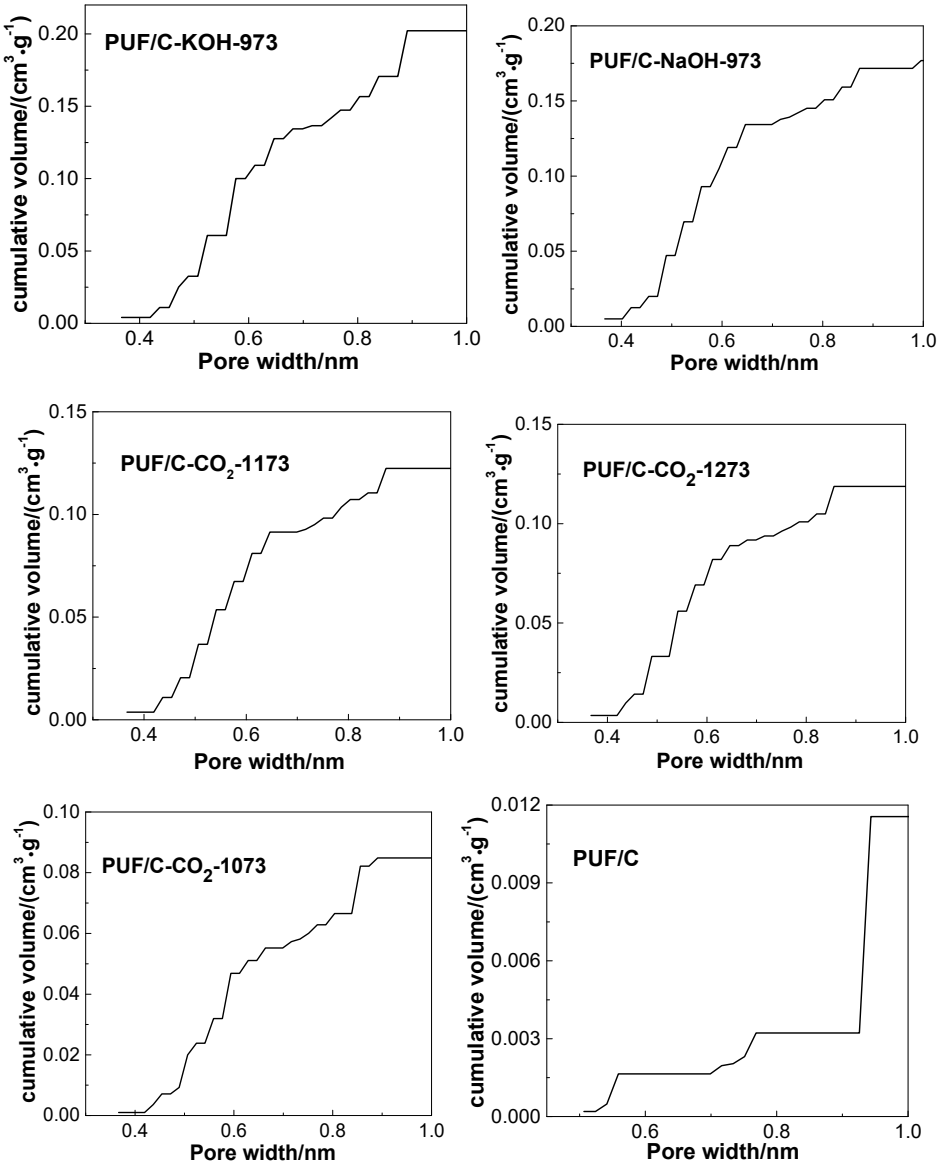

Figure 8. Cumulative volumes of ultramicropores (≤1 nm) calculated by the nonlocal density functional theory (NLDFT) method of PUF-based activated carbons. Adapted with permission from [15]. Copyright 2016 American Chemical Society.

In addition, the textural parameters of chemical activation samples are also shown in Table 2. The carbonized precursor was activated by chemical reagents $Ca(OH)_2$, NaOH, and KOH at 973 K. In addition to the sharp increase of surface area and pore volume from 39 $m^2 \cdot g^{-1}$ and 0.04 $cm^3 \cdot g^{-1}$ to 1360 $m^2 \cdot g^{-1}$ and 0.59 $cm^3 \cdot g^{-1}$, respectively, and the volumes of ultra-micropores (<1 nm) increased from barely detectable to 0.212 $cm^3 \cdot g^{-1}$ (Table 2 and Figure 8). It can be inferred that the pore structure of the carbon adsorbents could also be controlled by adjusting the chemical activation degree, and that increasing the degree of chemical activation is helpful for the formation of pores, especially the ultra-micropores, although a small number of mesopores were generated simultaneously.

Comparing physical activation with chemical activation, it can be concluded that physical activation mainly develops micropores and results in porous carbon materials with lower textural properties, which may affect the adsorption performance and lead to lower CO_2 uptake. However, it involves less contaminant, which avoids the emission of metal ions and the corrosion of equipment.

By increasing the activation temperature from 1073 to 1273 K (Table 2), the yield of porous carbons with physical activation decreased from 16% to 9.3%, as a result of CO_2 gas reacting with the walls of the pores (Equation (1)) [34]. In addition, the higher the burn-off temperature, the wider the pore size distribution becomes, as mentioned above. Regardless, higher carbon yield can be produced by physical activation due to lower burn-off degrees compared with effective chemical activation.

$$CO_2 + C \rightarrow 2CO \quad (1)$$

Similarly, the yield of carbon materials, as expected, decreased from 25.5% to 12.3% when enhancing the chemical activation degree using $Ca(OH)_2$, NaOH, or KOH as activated reagents (Table 2), which can be explained by graphitic C being oxidized by KOH beginning at 673 K, while for NaOH the temperature needs to be higher than 843 K, not even mentioning $Ca(OH)_2$ [35].

The porosity formed upon KOH, NaOH, and $Ca(OH)_2$ activation is considered to be the intercalation of metallic K, Na, and Ca in the carbon matrix, causing the deformation and expansion of the carbon lattice [36]. CO_2, H_2O, and H_2 generated in the redox reaction (take KOH and C for example) can also contribute to the development of pores. As shown in Equations (2)–(4) [35].

$$4KOH + C \rightarrow 4K + CO_2 + 2H_2O \quad (2)$$

$$4KOH + 2CO_2 \rightarrow 2K_2CO_3 + 2H_2O \quad (3)$$

$$6KOH + 2C \rightarrow 2K + 3H_2 + 2K_2CO_3 \quad (4)$$

3.4. CO_2 Adsorption Performances

CO_2 adsorption performances of samples with physical and chemical activation at 273 K are shown in Figure 9. For physically-activated samples, CO_2 adsorption capacities increased from 2.4 to 3.4 $mmol \cdot g^{-1}$ upon increasing activation temperature from 1073 to 1173 K. This cannot be simply attributed to surface area and pore volume (Table 2), since PUF/C-CO_2-1273 possesses larger surface area and pore volume but a lower CO_2 adsorption capacity than that of PUF/C-CO_2-1173. It was reported recently that small micropores are dominant in CO_2 capture for activated carbon materials [9]. This is attributed to the fact that the interaction between CO_2 and carbon adsorbents can be enhanced in small pores, especially at elevated temperatures and low pressures. The correlation of CO_2 uptake of PUF-based activated carbons at 273 K and 1 bar with the volumes of micropores (<1 nm) is presented in Figure 10a. Clearly, the CO_2 adsorption capacity shows a perfect linear correlation with the volumes of micropores less than 1 nm. Severe activation at higher temperature results in widening the pore size distribution, reducing the amount of ultra-micropores, which is responsible for the lower CO_2 uptake of PUF/C-CO_2-1273 compared to PUF/C-CO_2-1173.

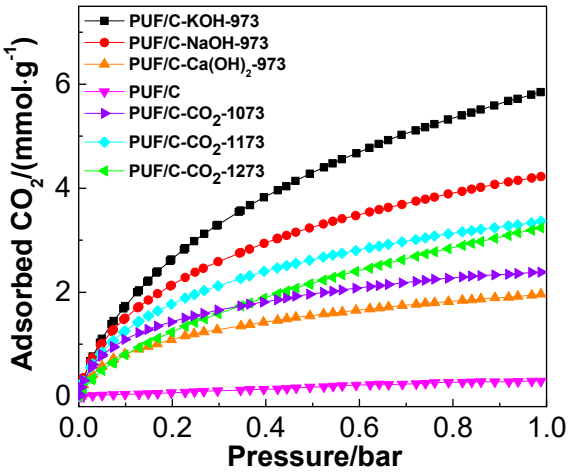

Figure 9. Adsorption isotherms of CO_2 at 273 K for the studied samples.

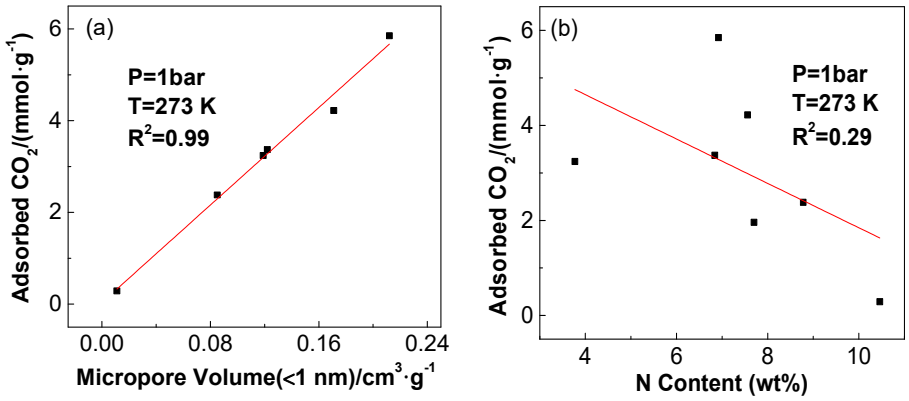

Figure 10. Correlation of CO_2 adsorption capacity with ultra-micropore volume (**a**) and with sample N content (**b**) at 273 K.

This trend can also be applied to the CO_2 adsorption performances of samples after chemical activation. Figure 8 shows that the adsorption capacity of CO_2 at 273 K and 1 bar increases as follows: PUF/C-Ca(OH)$_2$-973 < PUF/C-NaOH-973 < PUF/C-KOH-973. The PUF/C-KOH-973 sample exhibits the highest CO_2 uptake at 5.85 mmol·g^{-1}. This is mainly due to it having the largest ultra-micropore volume (<1 nm) of 0.212 cm^3·g^{-1} coupled with the largest surface area, pore volume, and abundance of basic N species. Chemical activation can be described by two steps: The formation of micropores, which is beginning with the redox reaction between activated agents and carbonized precursors; and the broadening of pores inside the opened porous channel [37]. Hence, the stage of creating micropores is primary when enhancing the activation degree from Ca(OH)$_2$ to KOH activation at 973 K.

N content in the prepared carbon materials may also contribute to the CO_2 adsorption capacity, wherein the correlation coefficient of CO_2 uptake with the N content (3.5–10.5 wt.%) of PUF-based activated carbons was only 0.29 (Figure 10b). This indicates that N content in the samples should not be the primary effect in this experiment. Thus, the superior CO_2 adsorption capabilities of the studied activated carbons predominantly result from the ultra-micropores (<1 nm).

Table 3 shows a comparation of CO_2 uptakes of carbon adsorbents prepared from PUF and other different waste materials at 273 K. It is worth mentioning that samples prepared with the waste polyurethane foams under CO_2 activation at 1173 K and KOH activation at 973 K exhibit comparable or better CO_2 adsorption capacities than those adsorbents obtained from many types of waste materials, such as ocean pollutant, sawdust, and coal fly ash (see Table 3). Whereas, some new derived activated carbons from biomass porous materials, like *Arundo donax* [29] or lotus seed [38], show a relatively

higher adsorption capacity. The results mentioned above suggest that activated carbon prepared from waste PUF is a potential candidate for use in capturing CO_2.

Table 3. CO_2 adsorption capacities at 273 K and 1 bar of activated carbons prepared from different waste materials.

Sample	CO_2 Adsorption Capacity (mmol·g^{-1}) at 273 K		Reference
	Physical Activation	Chemical Activation	
Spent coffee grounds activated carbons	3.5	4.8	[39]
Sawdust-based porous carbons	-	5.8	[40]
Coal-based carbon foams activated by $ZnCl_2$	-	3.4	[41]
CO_2 adsorbents based on ocean pollutant	-	2.4	[42]
Coal fly ash based materials	-	5	[43]
Macroalgae based N-doped carbons	-	3.06	[44]
Arundo donax-based activated bio-carbons	-	6.3	[29]
Biomass-derived activated porous bio-carbons	-	6.8	[38]
Polyurethane foam-based activated carbons	3.37	5.85	This work

3.5. CO_2 Adsorption Recyclability and Selectivity

CO_2 and N_2 adsorption behaviors of PUF/C-CO_2-1173 and PUF/C-KOH-973 at 273 K were compared, as shown in Figure 11. The N_2 adsorption capacity is 0.59 mmol g^{-1}, which is almost one-tenth of the CO_2 uptake of chemically-activated sample PUF/C-KOH-973. While, the selectivity of CO_2/N_2 of PUF/C-CO_2-1173 outperforms PUF/C-KOH-973 with a lower N_2 adsorption of only 0.14 mmol g^{-1} at 273 K, which is much higher than CO_2 adsorbents from other waste materials, such as mangosteen peel waste (24 vs. 12) [45]. This can be ascribed to the rich and narrower microporosity [39], as well as the nitrogen content of 6.84 wt% and the presence of other functional groups [46].

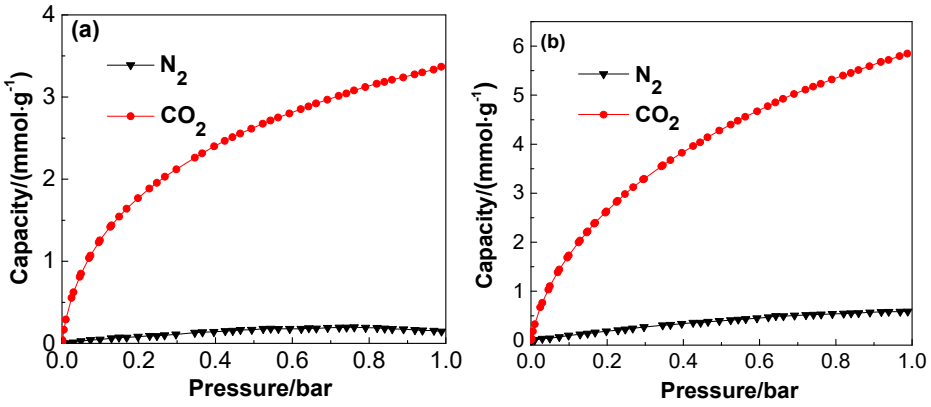

Figure 11. CO_2 and N_2 adsorption isotherms at 273 K on the PUF/C-CO_2-1173 (**a**) and PUF/C-KOH-973 (**b**).

The CO_2 adsorption performances of PUF/C-CO_2-1173 at 273 K and PUF/C-KOH-973 at 298 K are completely the same in the four repeated runs, as shown in Figure 12a,b, indicating that the physically-activated sample has as high of a recyclability as the chemically-activated sample. Hence, in comparison with the environmental pollution and cumbersome process associated with chemical activation, CO_2 sorbent from waste polyurethane foam by physical activation is encouraged, due to the higher CO_2/N_2 selectivity and the relatively higher carbon yield.

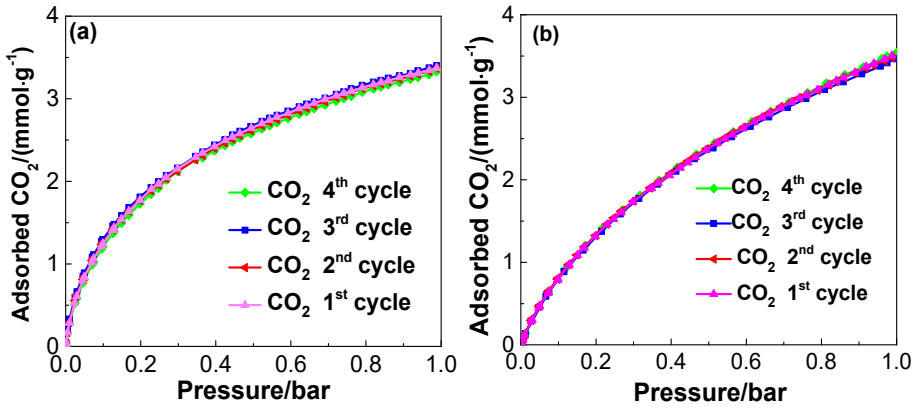

Figure 12. CO_2 adsorption performances on the PUF/C-CO_2-1173 at 273 K (**a**) and PUF/C-KOH-973 at 298 K (**b**) within four repeated cycles with regeneration.

4. Conclusions

In this work, waste polyurethane foam was physically activated by CO_2 for the first time and chemically activated with $Ca(OH)_2$, NaOH, or KOH, and was compared for the preparation of the low-cost activated carbons with a highly-developed porosity. To achieve high CO_2 adsorption capacity and CO_2/N_2 selectivity, activation conditions of the waste polyurethane foam were optimized. The low CO_2 flowrate (15 mL·min^{-1}) and temperature of 1173 K for CO_2 activation are beneficial to the formation of a narrower microporosity. This, combined with relatively high nitrogen content, resulted in the high CO_2/N_2 selectivity of up to 24, much higher than samples that underwent chemical activation. However, physical activation samples showed inferior textural properties compared to chemical activation samples and led to lower CO_2 uptake. The sample activated with KOH possessed a high volume of ultramicropores (<1 nm) and surface area up to 0.212 cm^3·g^{-1} and 1360 m^2·g^{-1}, respectively. A high CO_2 adsorption capacity of 5.85 mmol·g^{-1} was obtained at 273 K and 1 bar, which was better than the physical activation sample with 3.37 mmol·g^{-1}, and is comparable to the best reported carbon materials prepared from other waste materials. Moreover, in consideration of the decreased presence of the contaminant, the lower weight losses of physical activation samples, and the excellent recyclability of both physical and chemical activated samples, the waste polyurethane foam-based carbon materials exhibited potential application prospects in CO_2 capture.

Author Contributions: Writing—original draft, C.G.; data curation, D.L.; investigation, S.C.; formal analysis, J.G.; supervision, J.L.

Funding: This research was funded by the National Natural Science Foundation of China (No. 21802101), Scientific and Technological Innovation Programs of Higher Education Institutions in Shanxi, and Shanxi Province Science Foundation for Youths (No. 201801D221129).

Conflicts of Interest: The authors declare no conflicts of interest.

References

1. Wang, J.; Heerwig, A.; Lohe, M.R.; Oschatz, M.; Borchardt, L.; Kaskel, S. Fungi-based porous carbons for CO_2 adsorption and separation. *J. Mater. Chem.* **2012**, *22*, 13911–13913. [CrossRef]
2. Schrag, D.P. Preparing to capture carbon. *Science* **2007**, *315*, 812–813. [CrossRef] [PubMed]
3. Morris, J.; Paltsev, S.; Ku, A.Y. Impacts of China's emissions trading schemes on deployment of power generation with carbon capture and storage. *Energy Econ.* **2019**, *81*, 848–858. [CrossRef]
4. Wilberforce, T.; Baroutaji, A.; Soudan, B.; Al-Alami, A.H.; Olabi, A.G. Outlook of carbon capture technology and challenges. *Sci. Total Environ.* **2019**, *657*, 56–72. [CrossRef] [PubMed]
5. Wang, S.; Li, W.C.; Zhang, L.; Jin, Z.Y.; Lu, A.H. Polybenzoxazine-based monodisperse carbon spheres with low-thermal shrinkage and their CO_2 adsorption properties. *J. Mater. Chem. A* **2014**, *2*, 4406–4412. [CrossRef]

6. Li, P.; Wang, Z.; Li, W.; Liu, Y.; Wang, J.; Wang, S. High-performance multilayer composite membranes with mussel-inspired polydopamine as a versatile molecular bridge for CO_2 separation. *ACS Appl. Mater. Interfaces* **2015**, *7*, 15481–15493. [CrossRef] [PubMed]
7. Du, N.; Park, H.B.; Robertson, G.P.; Dal-Cin, M.M.; Visser, T.; Scoles, L.; Guiver, M.D. Polymer nanosieve membranes for CO_2-capture applications. *Nat. Mater.* **2011**, *10*, 372–375. [CrossRef]
8. Bae, Y.S.; Snurr, R.Q. Development and Evaluation of Porous Materials for Carbon Dioxide Separation and Capture. *Angew. Chem. Int. Ed.* **2011**, *50*, 11586–11596. [CrossRef]
9. Su, F.; Lu, C. CO_2 capture from gas stream by zeolite 13X using a dual-column temperature/vacuum swing adsorption. *Energy Environ. Sci.* **2012**, *5*, 9021–9027. [CrossRef]
10. Khan, I.U.; Othman, M.H.D.; Ismail, A.; Ismail, N.; Jaafar, J.; Hashim, H.; Rahman, M.A.; Jilani, A. Structural transition from two-dimensional ZIF-L to three-dimensional ZIF-8 nanoparticles in aqueous room temperature synthesis with improved CO_2 adsorption. *Mater. Charact.* **2018**, *136*, 407–416. [CrossRef]
11. Yu, H.; Wang, X.; Shu, Z.; Fujii, M.; Song, C. Al_2O_3 and CeO_2-promoted MgO sorbents for CO_2 capture at moderate temperatures. *Front. Chem. Sci. Eng.* **2018**, *12*, 83–93. [CrossRef]
12. Chandra, V.; Yu, S.U.; Kim, S.H.; Yoon, Y.; Kim, D.Y.; Kwon, A.H.; Meyyappan, M.; Kim, K.S. Highly selective CO_2 capture on N-doped carbon produced by chemical activation of polypyrrole functionalized graphene sheets. *Chem. Commun.* **2012**, *48*, 735–737. [CrossRef] [PubMed]
13. Gu, J.M.; Kim, W.S.; Hwang, Y.K.; Huh, S. Template-free synthesis of N-doped porous carbons and their gas sorption properties. *Carbon* **2013**, *56*, 208–217. [CrossRef]
14. Song, J.; Shen, W.; Wang, J.; Fan, W. Superior carbon-based CO_2 adsorbents prepared from poplar anthers. *Carbon* **2014**, *69*, 255–263. [CrossRef]
15. Ge, C.; Song, J.; Qin, Z.; Wang, J.; Fan, W. Polyurethane Foam-Based Ultramicroporous Carbons for CO_2 Capture. *ACS Appl. Mater. Interfaces* **2016**, *8*, 18849–18859. [CrossRef] [PubMed]
16. Zhang, Z.; Zhou, J.; Xing, W.; Xue, Q.; Yan, Z.; Zhuo, S.; Qiao, S.Z. Critical role of small micropores in high CO_2 uptake. *Phys. Chem. Chem. Phys.* **2013**, *15*, 2523–2529. [CrossRef]
17. Ello, A.S.; De Souza, L.K.; Trokourey, A.; Jaroniec, M. Coconut shell-based microporous carbons for CO_2 capture. *Microporous Mesoporous Mater.* **2013**, *180*, 280–283. [CrossRef]
18. Heo, Y.J.; Park, S.J. H_2O_2/steam activation as an eco-friendly and efficient top-down approach to enhancing porosity on carbonaceous materials: The effect of inevitable oxygen functionalities on CO_2 capture. *Green Chem.* **2018**, *20*, 5224–5234. [CrossRef]
19. Prauchner, M.J.; Rodríguez-Reinoso, F. Chemical versus physical activation of coconut shell: A comparative study. *Microporous Mesoporous Mater.* **2012**, *152*, 163–171. [CrossRef]
20. Sevilla, M.; Fuertes, A.B.; Solis, M.S.; Valle-Vigón, P. N-Doped Polypyrrole-Based Porous Carbons for CO_2 Capture. *Adv. Funct. Mater.* **2011**, *21*, 2781–2787. [CrossRef]
21. Nandi, M.; Okada, K.; Dutta, A.; Bhaumik, A.; Maruyama, J.; Derks, D.; Uyama, H. Unprecedented CO_2 uptake over highly porous N-doped activated carbon monoliths prepared by physical activation. *Chem. Commun.* **2012**, *48*, 10283–10285. [CrossRef] [PubMed]
22. Meng, F.Z.; Gong, Z.Q.; Wang, Z.B.; Fang, P.W.; Li, X.Y. Study on a nitrogen-doped porous carbon from oil sludge for CO_2 adsorption. *Fuel* **2019**, *251*, 562–571. [CrossRef]
23. Agrawal, A.; Kaur, R.; Walia, R. PU foam derived from renewable sources: Perspective on properties enhancement: An overview. *Eur. Polym. J.* **2017**, *95*, 255–274. [CrossRef]
24. Shinko, A. Introduction to Mechanical Recycling and Chemical Depolymerization. *Recycl. Polyurethane Foam.* **2018**, *4*, 45–55.
25. Sheel, A.; Pant, D. Chemical Depolymerization of Polyurethane Foams via Glycolysis and Hydrolysis. *Recycl. Polyurethane Foam.* **2018**, *6*, 67–75.
26. Padhan, R.K. Chemical Depolymerization of Polyurethane Foams via Combined Chemolysis Methods. *Recycl. Polyurethane Foam.* **2018**, *8*, 89–96.
27. Quadrini, F.; Bellisario, D.; Santo, L. Recycling of thermoset polyurethane foams. *Polym. Eng. Sci.* **2013**, *53*, 1357–1363. [CrossRef]
28. Ferdan, T.; Pavlas, M.; Nevrlý, V.; Šomplák, R.; Stehlík, P. Greenhouse gas emissions from thermal treatment of non-recyclable municipal waste. *Front. Chem. Sci. Eng.* **2018**, *12*, 815–831. [CrossRef]

29. Singh, G.; Kim, I.Y.; Lakhi, K.S.; Srivastava, P.; Naidu, R.; Vinu, A. Single step synthesis of activated bio-carbons with a high surface area and their excellent CO_2 adsorption capacity. *Carbon* **2017**, *116*, 448–455. [CrossRef]
30. Pevida, C.; Drage, T.; Snape, C.; Drage, T.; Snape, C. Silica-templated melamine–formaldehyde resin derived adsorbents for CO_2 capture. *Carbon* **2008**, *46*, 1464–1474. [CrossRef]
31. Su, F.; Poh, C.K.; Chen, J.S.; Xu, G.; Wang, D.; Li, Q.; Lin, J.; Lou, X.W. Nitrogen-containing microporous carbon nanospheres with improved capacitive properties. *Energy Environ. Sci.* **2011**, *4*, 717–724. [CrossRef]
32. Hao, G.P.; Li, W.C.; Qian, D.; Lu, A.H. Rapid Synthesis of Nitrogen-Doped Porous Carbon Monolith for CO_2Capture. *Adv. Mater.* **2010**, *22*, 853–857. [CrossRef] [PubMed]
33. Martín, C.; Plaza, M.; Pis, J.; Rubiera, F.; Pevida, C.; Centeno, T.A. On the limits of CO_2 capture capacity of carbons. *Sep. Purif. Technol.* **2010**, *74*, 225–229. [CrossRef]
34. Chaudhary, A.; Kumari, S.; Kumar, R.; Teotia, S.; Singh, B.P.; Singh, A.P.; Dhawan, S.K.; Dhakate, S.R. Lightweight and easily foldable MCMB-MWCNTs composite paper with exceptional electromagnetic interference shielding. *ACS Appl. Mater. Interface* **2016**, *8*, 10600–10608. [CrossRef] [PubMed]
35. Lillo-Ródenas, M.A.; Cazorla-Amorós, D.; Linares-Solano, A. Understanding chemical reactions between carbons and NaOH and KOH: An insight into the chemical activation mechanism. *Carbon* **2003**, *41*, 267–275. [CrossRef]
36. Dıaz-Terán, J.; Nevskaia, D.; Fierro, J.; Lopez-Peinado, A.J.; Jerez, A. Study of chemical activation process of a lignocellulosic material with KOH by XPS and XRD. *Microporous Mesoporous Mater.* **2003**, *60*, 173–181.
37. Rodriguez-Reinoso, F.; Molina-Sabio, M. Activated carbons from lignocellulosic materials by chemical and/or physical activation: An overview. *Carbon* **1992**, *30*, 1111–1118. [CrossRef]
38. Singh, G.; Lakhi, K.S.; Ramadass, K.; Sathish, C.I.; Vinu, A. High-performance biomass-derived activated porous biocarbons for combined pre- and post-combustion CO_2 capture. *ACS Sustain. Chem. Eng.* **2019**, *7*, 7412–7420. [CrossRef]
39. Plaza, M.; Gonzalez, A.; Pevida, C.; Pis, J.; Rubiera, F. Valorisation of spent coffee grounds as CO_2 adsorbents for postcombustion capture applications. *Appl. Energy* **2012**, *99*, 272–279. [CrossRef]
40. Sevilla, M.; Fuertes, A.B. Sustainable porous carbons with a superior performance for CO_2 capture. *Energy Environ. Sci.* **2011**, *4*, 1765–1771. [CrossRef]
41. Rodríguez, E.; García, R. Low-cost hierarchical micro/macroporous carbon foams as efficient sorbents for CO_2 capture. *Fuel Process. Technol.* **2017**, *156*, 235–245. [CrossRef]
42. Zhang, Z.; Wang, K.; Atkinson, J.D.; Yan, X.; Li, X.; Rood, M.J.; Yan, Z. Sustainable and hierarchical porous Enteromorpha prolifera based carbon for CO_2 capture. *J. Hazard. Mater.* **2012**, *229*, 183–191. [CrossRef] [PubMed]
43. Liu, L.; Singh, R.; Xiao, P.; Webley, P.A.; Zhai, Y. Zeolite synthesis from waste fly ash and its application in CO_2 capture from flue gas streams. *Adsorption* **2011**, *17*, 795–800. [CrossRef]
44. Ren, M.; Zhang, T.; Wang, Y.; Jia, Z.; Cai, J. A highly pyridinic N-doped carbon from macroalgae with multifunctional use toward CO_2 capture and electrochemical applications. *J. Mater. Sci.* **2018**, *54*, 1606–1615. [CrossRef]
45. Li, Y.; Wang, X.; Cao, M. Three-dimensional porous carbon frameworks derived from mangosteen peel waste as promising materials for CO_2 capture and supercapacitors. *J. CO_2 Util.* **2018**, *27*, 204–216. [CrossRef]
46. Zhai, Q.G.; Bai, N.; Li, S.; Bu, X.; Feng, P. Design of Pore Size and Functionality in Pillar-Layered Zn-Triazolate-Dicarboxylate Frameworks and Their High CO_2/CH_4 and C_2 Hydrocarbons/CH_4 Selectivity. *Inorg. Chem.* **2015**, *54*, 9862–9868. [CrossRef] [PubMed]